

# De novo synthesis of a metal–organic framework material featuring ultrahigh surface area and gas storage capacities

Omar K. Farha<sup>1</sup>, A. Özgür Yazaydın<sup>2</sup>, Ibrahim Eryazici<sup>1</sup>, Christos D. Malliakas<sup>1</sup>, Brad G. Hauser<sup>1</sup>, Mercouri G. Kanatzidis<sup>1</sup>, SonBinh T. Nguyen<sup>1</sup>, Randall Q. Snurr<sup>2\*</sup> and Joseph T. Hupp<sup>1\*</sup>

**Metal–organic frameworks—a class of porous hybrid materials built from metal ions and organic bridges—have recently shown great promise for a wide variety of applications. The large choice of building blocks means that the structures and pore characteristics of the metal–organic frameworks can be tuned relatively easily. However, despite much research, it remains challenging to prepare frameworks specifically tailored for particular applications. Here, we have used computational modelling to design and predictively characterize a metal–organic framework (NU-100) with a particularly high surface area. Subsequent experimental synthesis yielded a material, matching the calculated structure, with a high BET surface area (6,143 m<sup>2</sup> g<sup>-1</sup>). Furthermore, sorption measurements revealed that the material had high storage capacities for hydrogen (164 mg g<sup>-1</sup>) and carbon dioxide (2,315 mg g<sup>-1</sup>)—gases of high importance in the contexts of clean energy and climate alteration, respectively—in excellent agreement with predictions from modelling.**

Metal–organic frameworks (MOFs) are an intriguing class of hybrid materials<sup>1–3</sup> that are built by assembling metal centres with organic linkers. Through judicious choice of components, materials with permanent nanoscale porosity can be prepared. Some of the most notable examples have large internal surface areas and ultralow densities, with uniform cavities and voids with pre-designed molecular dimensions. Among the many potential applications that can be extrapolated from these properties are gas storage<sup>4–11</sup>, molecular separation<sup>12</sup>, chemical catalysis<sup>13,14</sup>, sensing<sup>15</sup>, ion exchange<sup>16</sup> and drug delivery<sup>17,18</sup>.

An important feature of these materials is their crystallinity. This allows for unambiguous structural determination to be made using X-ray diffraction measurements. This information about the precise molecular structure makes it possible to use highly accurate computational modelling of the static and dynamic interactions of guest molecules in the MOF pores to calculate adsorption isotherms, binding energies and transport behaviour, in both predictive and explanative modes<sup>19–21</sup>. Such computational studies can be used, for example, to design and screen MOFs regarding their potential surface areas and effective capacities for storage applications. In this report, we demonstrate how computational design can be used as a powerful tool for identifying promising MOFs before experimentally synthesizing them. This approach should aid researchers by enabling them to narrow the possible synthesis targets to MOFs with high potential for success in specific applications. Based on this strategy, we have experimentally synthesized a new MOF displaying high gas storage capacities and one of the highest reported surface areas to date.

## Results and discussion

Several topologies were initially considered in the design process, with a (3,24)-paddlewheel connected network ultimately being chosen. There were three reasons for this choice. First, it was antici-

pated that this topology would have high stability under ambient conditions (including in the presence of moisture)<sup>22–24</sup>. Second, it has ‘open’ coordination sites (unsaturated Cu(II) sites), which have been shown to enhance gas uptake in low-pressure regimes by favourably interacting with sorbate molecules<sup>25,26</sup>. Finally, interpenetration was impossible. Network interpenetration occurs when two or more independent, identical network are entangled, partially filling each other’s pores, and they cannot be separated without breaking bonds. Avoiding this ensures that the maximum surface area for a given material is achieved. Additionally, we chose this topology because it provides cavities of different sizes within the same MOF. This is an important feature that can be used to advantage for storage applications spanning a wide range of pressures<sup>27</sup>. MOFs with this topology were recently synthesized by Yan and colleagues<sup>24</sup> and Zhou and colleagues<sup>28</sup>. They incorporated the above properties by connecting the 24 edges of a cuboctahedron (or the 24 corners of a rhombicuboctahedron) with linkers having C<sub>3</sub> symmetry.

**Computational modelling.** In this Article, we have designed and synthesized a MOF with an ultrahigh surface area and high storage capacities for hydrogen and carbon dioxide, which is based on a hexatopic carboxylate ligand (LH<sub>6</sub>; **10**, shown in Fig. 1a). The design of this material was carried out *in silico* using Materials Studio Visualizer<sup>29</sup> to predictively characterize its structure, surface area and storage capacity. This was done by replacing the ligand used by Yan and colleagues<sup>24</sup> with LH<sub>6</sub>, while using the same copper paddlewheel cluster and cubic space group (*Fm*  $\bar{3}$  *m*) to ensure the same (3,24)-paddlewheel topology.

After creation of the initial structure, its geometry was refined by a self-consistent iterative procedure in which successive geometry optimization calculations were performed using the Forcite module of Materials Studio<sup>29</sup>, until differences between the dimensions of two successive unit cells were smaller than 0.001 Å. The

<sup>1</sup>Department of Chemistry and International Institute for Nanotechnology, Northwestern University, 2145 Sheridan Road, Evanston, Illinois 60208, USA,

<sup>2</sup>Department of Chemical and Biological Engineering, Northwestern University, 2145 Sheridan Road, Evanston, Illinois 60208, USA.

\*e-mail: j-hupp@northwestern.edu; snurr@northwestern.edu

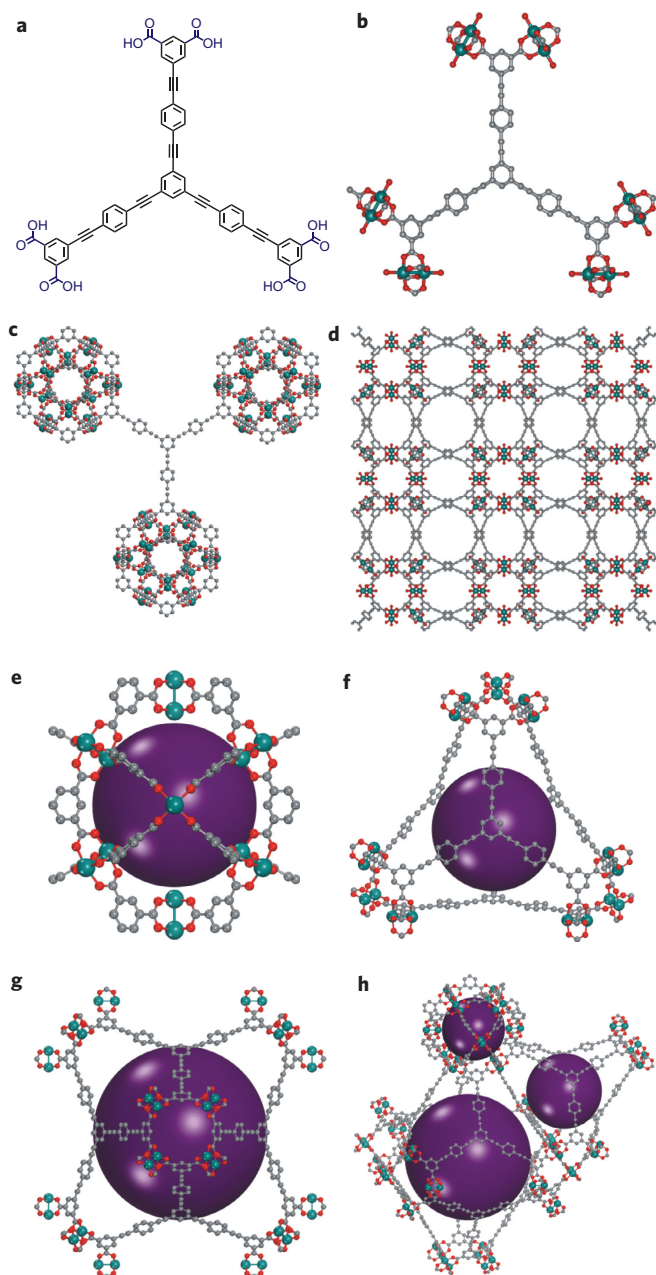


**Figure 1 | Structural features of NU-100.** **a**, Schematic of the chemical structure of  $\text{LH}_6$ . **b–h**, Representations of the single-crystal X-ray structure of **NU-100**:  $\text{LH}_6$  connecting six paddlewheel units (**b**), cubaoctahedral building blocks (**c**) and different cages in **NU-100** (**e–h**). Hydrogens and disordered solvent molecules are omitted for clarity. Carbon, grey; oxygen, red; copper, teal. Purple, representation of the largest spheres that can fit within the cages.

geometry optimization was based on classical molecular mechanics calculations, where the energies between the atoms were calculated by applying a model that consisted of both bonded and non-bonded potentials. The potential between bonded atoms and the short-range part of the non-bonded potential (van der Waals interactions) were modelled using the Universal Force Field<sup>30</sup>. The long-range part of the non-bonded potential (electrostatic interactions) was modelled using partial charges on the framework atoms. Before each run, new partial atomic charges were derived by using density functional theory calculations, because the charges depend on the coordinates of the atoms relative to each other (see

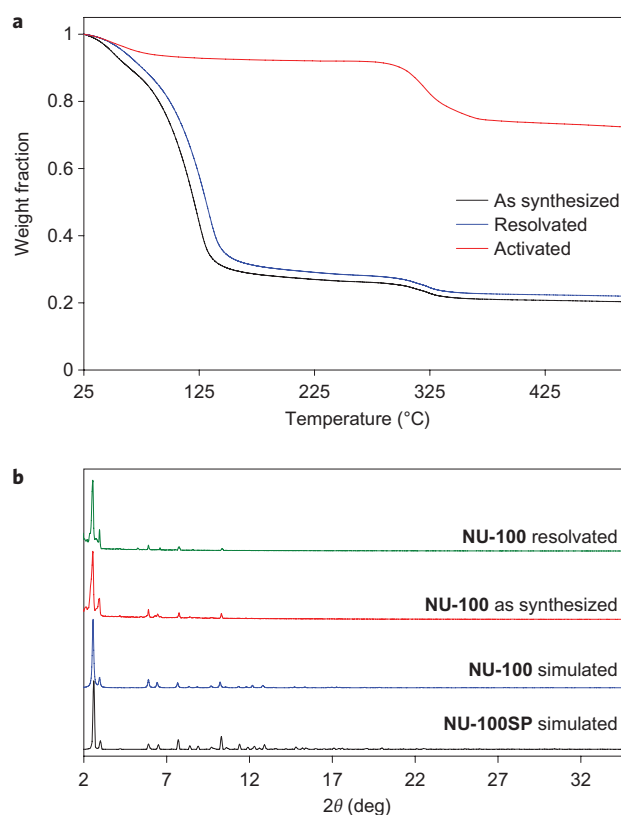


**Figure 2 | TGA and PXRD profiles.** **a**, TGA profiles of **NU-100**. The two weight loss steps correspond to free solvent and decomposition of the material, respectively. **b**, PXRD patterns for **NU-100** and **NU-100SP**. PXRD patterns show the good agreement between the simulated and experimental structures, and between the as-synthesized and resolved materials, which shows that the framework retains its crystallinity.

Supplementary Information for further details of the geometry optimization procedure).

Once the final refined structure was obtained, we calculated its BET surface area<sup>21</sup> based on a simulated  $\text{N}_2$  adsorption isotherm (see Supplementary Information.) The BET surface area of the predicted structure (**NU-100SP**) (where **NU** and **SP** stand for ‘Northwestern University’ and ‘simulation predicted’, respectively) was calculated to be  $6,605 \text{ m}^2 \text{ g}^{-1}$ . This calculated ultrahigh surface area motivated us to proceed with the experiments, starting with the large-scale synthesis of the new hexacarboxylic acid species ( $\text{LH}_6$ ; **10**, see Supplementary Section S1 and Fig. 1a) via a series of coupling and deprotection reactions (see Supplementary Information). The expectation was that the deprotonated form of  $\text{LH}_6$  (**10**), when combined with appropriate metal ions, would form the predicted structure through coordination of the carboxylate groups. While this work was in review, a related paper by Yuan and colleagues appeared<sup>28</sup>. Several new MOFs were reported, including **PCN-610**, which is identical to the unactivated (that is, solvent-filled) form of **NU-100**. Difficulties in activating **PCN-610** prevented its surface area and sorption properties from being experimentally investigated, although a comprehensive experimental study of related MOFs, featuring smaller cavities, was reported.

**Synthesis and characterization.** A solvothermal reaction of  $\text{LH}_6$  (**10**) and  $\text{Cu}(\text{NO}_3)_2 \cdot 2.5\text{H}_2\text{O}$  in  $\text{DMF}/\text{HBF}_4$  at  $75^\circ\text{C}$  for 24 h afforded a MOF having the framework formula  $[\text{Cu}_3(\text{L})(\text{H}_2\text{O})_3]_n$  (**NU-100/PCN-610**) ( $\text{DMF}$ , dimethylformamide). X-ray analysis of a single crystal of **NU-100** revealed a non-catenated structure (that is, non-interpenetrated), in which the framework

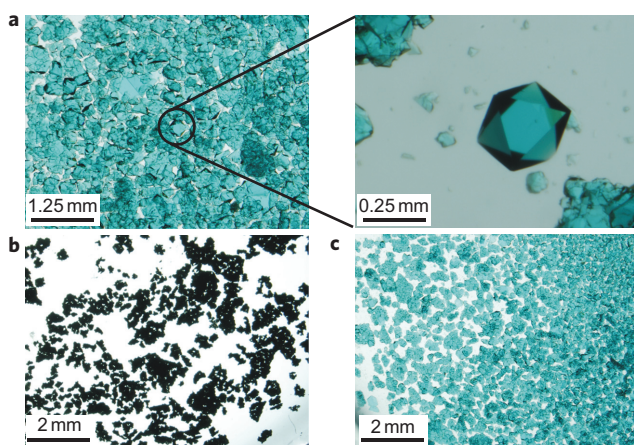


**Figure 3 | Photographic images of NU-100.** **a**, Crystals of as-synthesized NU-100 (right panel shows an enlarged image). **b**, Resolvated NU-100 in DMF after an unsuccessful activation procedure (that is, not using supercritical CO<sub>2</sub>), showing its collapsed morphology. **c**, Resolvated NU-100 in DMF after activation with supercritical CO<sub>2</sub>.

nodes consist of Cu(II)<sub>2</sub> units coordinated by the carboxylates of **L** in a paddlewheel fashion. The axial sites of the Cu(II)<sub>2</sub> units are ligated by water molecules (Fig. 1). The pores of the MOF are filled with disordered solvent molecules. Thermogravimetric analysis (TGA) of NU-100 revealed a mass loss at about 125 °C, assigned to the loss of solvent (DMF), with no further mass loss occurring until 325 °C, at which point the material decomposes (Fig. 2a).

The purity of the bulk material was confirmed by powder X-ray diffraction (PXRD) measurements (Fig. 2b). More importantly, the

experimental structure, NU-100, was found to be nearly identical to the predicted structure, NU-100SP. Comparison of the diffraction data of the predicted structure and the experimental structure revealed differences of less than 0.4 Å in the unit cell dimensions, supporting the viability of the *in silico* approach to screening MOF structures. The predicted structure has unit cell dimensions of  $a = b = c = 59.539$  Å at 0 K, and the experimental cell has dimensions of  $a = b = c = 59.872(2)$  Å at 100 K.

The pore size distribution of NU-100, calculated from argon adsorption experiments at 87 K using non-local density functional theory (NLDFT), revealed peaks at 17, 24 and 30 Å (see Supplementary Information). NU-100 has three types of cavities. The largest spheres that can fit in these cavities, based on the van der Waals surface of the framework interior, were computed to be 13.4, 15.4 and 27.4 Å in diameter (Fig. 1e–h) using the method of Gelb and Gubbins<sup>31</sup>, which is in good agreement with the sorption-based pore size analysis. The largest open cage length in this MOF is 48 Å (~5 nm).

For most applications and in particular for gas storage, it is highly desirable to remove guest solvent molecules from the pores of the MOF without significantly diminishing porosity. If the porosity is partially or completely lost, significant discrepancies will arise between the surface areas that are obtained experimentally and those estimated from computational studies. Furthermore, MOFs containing large pores (mesopores), including NU-100, are particularly susceptible to incomplete activation (that is, only partial removal of guest molecules from the pores). We applied many activation procedures and found that only activation with supercritical carbon dioxide (SCD) was able to remove guest solvent molecules without damaging NU-100<sup>32</sup>. SCD processing was performed with a Tousimi Samdri PVT-30 critical point dryer. Before SCD drying, DMF-solvated MOF samples were soaked in absolute

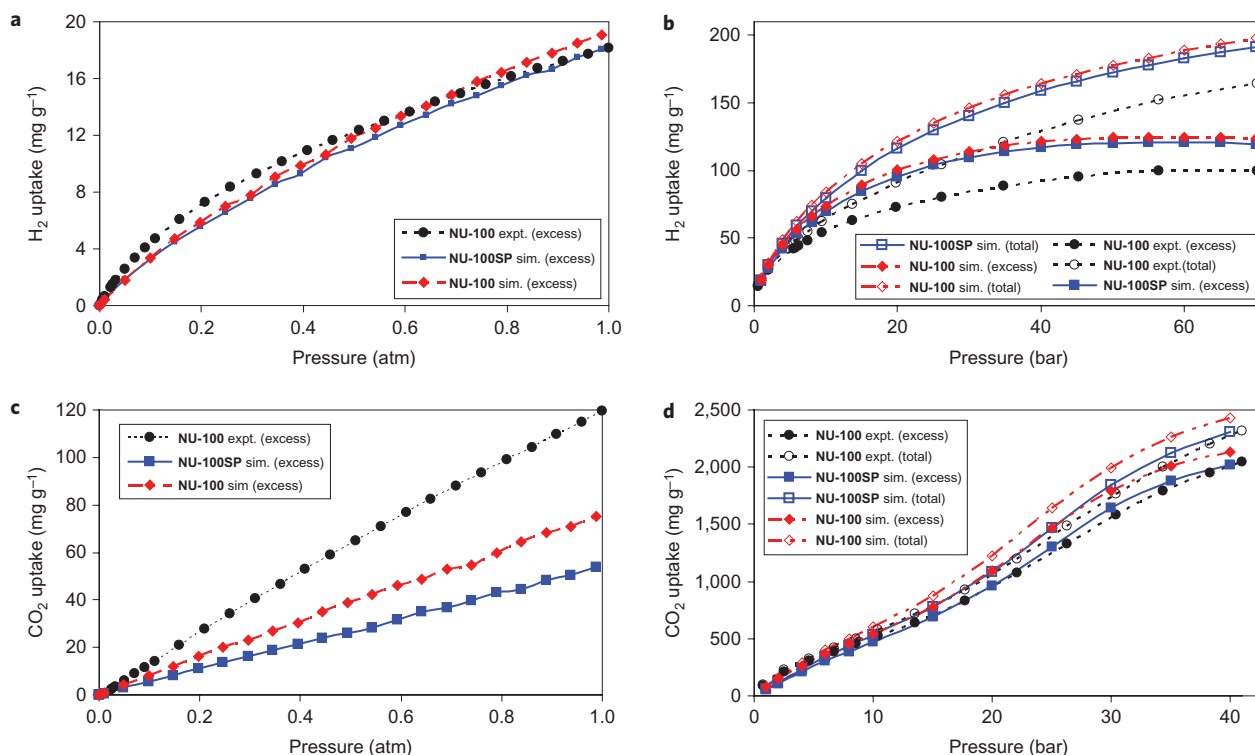


**Figure 4 | Sorption data for the simulated and synthesized NU-100.** **a–d**, Experimental gas sorption data for NU-100 (black circles), simulated gas sorption data for NU-100SP (blue squares) and simulated data gas sorption for NU-100 (red diamonds) with low-pressure H<sub>2</sub> (77 K) (**a**), high-pressure H<sub>2</sub> (77 K) (**b**), low-pressure CO<sub>2</sub> (298 K) (**c**) and high-pressure CO<sub>2</sub> (298 K) (**d**). Filled symbols represent excess uptake and empty symbols represent total uptake. Total uptake for experiments and excess uptake for simulations were calculated using the formula  $N_{\text{total}} = N_{\text{excess}} + \rho_{\text{gas}} \cdot V_p$ , where  $\rho_{\text{gas}}$  is the bulk density of the gas<sup>32</sup> and  $V_p$  is the pore volume.

**Table 1 | Surface area and gas sorption data for high surface area MOF materials.**

MOF	Expt. BET SA (m <sup>2</sup> g <sup>-1</sup> )	Sim. BET SA (m <sup>2</sup> g <sup>-1</sup> )	Excess H <sub>2</sub> uptake* (mg g <sup>-1</sup> )	Total H <sub>2</sub> uptake <sup>†</sup> (mg g <sup>-1</sup> )	Excess CO <sub>2</sub> uptake <sup>‡</sup> (mg g <sup>-1</sup> )	Total CO <sub>2</sub> uptake <sup>§</sup> (mg g <sup>-1</sup> )
MOF-5 <sup>7,40</sup>	3,800	3,527	76	108	968	1,072
NOTT-112 <sup>24</sup>	3,800	4,286	76	105	NA	NA
MOF-177 <sup>8,40</sup>	4,740	4,948	73	115	1493	1,656
UMCM-2 <sup>9</sup>	5,200	5,583	69	116	NA	NA
MOF-210 <sup>33</sup>	6,240	6,580	86	167	2,396	2,480
NU-100	6,143	6,515	99.5	164	2,043	2,315

\*Maximum value reported at 77 K. <sup>†</sup>At 70 bar and 77 K. <sup>‡</sup>Maximum value reported at 298 K. <sup>§</sup>At 40 bar and 298 K. SA, surface area; Expt., experimental; Sim., simulation.

ethanol for 3 days, with the soaking solution being replaced every 24 h. After soaking, the ethanol-containing samples were placed inside the dryer and the ethanol was exchanged with CO<sub>2</sub>(liq.) over a period of 10 h. The temperature was then raised and CO<sub>2</sub> was vented under supercritical conditions. Follow-up TGA experiments showed that NU-100 was fully evacuated and resolvated, while PXRD data and crystal images revealed that the resolvated form retained its crystallinity (Figs 2b and 3).

**Sorption capabilities.** The porosity of activated NU-100 was examined via N<sub>2</sub> adsorption at 77 K. The experimental BET surface area of activated NU-100 was found to be 6,143 m<sup>2</sup> g<sup>-1</sup>, in excellent agreement with its simulated BET surface area (6,515 m<sup>2</sup> g<sup>-1</sup>) and with the simulated BET surface area of NU-100SP (6,605 m<sup>2</sup> g<sup>-1</sup>). This surface area is one of the highest reported to date for any porous material. The largest, to our knowledge, is 6,240 m<sup>2</sup> g<sup>-1</sup> for the very recently reported material, MOF-210<sup>33</sup>. The total pore volume of NU-100 is 2.82 cm<sup>3</sup> g<sup>-1</sup>, which is substantially larger than those of nearly all other high-pore-volume MOFs, including MOF-5 (1.55 cm<sup>3</sup> g<sup>-1</sup>)<sup>7</sup>, NOTT-112 (1.62 cm<sup>3</sup> g<sup>-1</sup>)<sup>24</sup>, MOF-177 (1.89 cm<sup>3</sup> g<sup>-1</sup>)<sup>8</sup>, MIL-101(Cr) (1.9 cm<sup>3</sup> g<sup>-1</sup>)<sup>34</sup>, PCN-68<sup>28</sup> (also known as NOTT-116<sup>35</sup>, 2.13 cm<sup>3</sup> g<sup>-1</sup>) and UMCM-2 (2.31 cm<sup>3</sup> g<sup>-1</sup>)<sup>9</sup>. At present, only MOF-210 appears to offer a larger pore volume (3.6 cm<sup>3</sup> g<sup>-1</sup>)<sup>33</sup>.

The large surface area and pore volume of NU-100 prompted us to measure its high-pressure hydrogen and carbon dioxide storage capacities. Sorption data were collected up to 70 bar at 77 K for H<sub>2</sub> and 40 bar at 298 K for CO<sub>2</sub>. It should be noted that only the 'excess' gas adsorption is directly accessible experimentally. Excess gas adsorption is the amount adsorbed due to the presence of the adsorbent. The 'total' adsorption is the sum of the excess adsorption and the amount that would be found within the pore volume even in the absence of the adsorbent, simply due to the finite bulk-phase density of the gas. For gas storage and delivery purposes, the total amount adsorbed is the more relevant quantity.

The excess hydrogen uptake of NU-100 was 18.2 mg g<sup>-1</sup> at 1 bar and 99.5 mg g<sup>-1</sup> at 56 bar (Fig. 4a,b). By using the N<sub>2</sub>-derived pore

volume (2.82 cm<sup>3</sup> g<sup>-1</sup>) and the bulk phase density of H<sub>2</sub> (ref. 36), the total H<sub>2</sub> uptake at 70 bar and 77 K was calculated to be 164 mg g<sup>-1</sup>. With the exception of the total value for MOF-210 (Table 1), these values substantially exceed any others reported for MOF materials. Furthermore, they position NU-100 within range of the US Department of Energy's revised long-term systems target for on-board H<sub>2</sub> storage, 7.5 wt% (=81 mg g<sup>-1</sup>), albeit at cryogenic rather than ambient temperature<sup>37</sup>. Variable-temperature measurements reveal an isosteric heat of adsorption of 6.1 kJ mol<sup>-1</sup> in the low-loading limit, presumably due to the availability of open Cu(II) coordination sites in NU-100. This value compares favourably with MOFs lacking special sorption sites; their heats of adsorption are typically in the 4–5 kJ mol<sup>-1</sup> range<sup>6</sup>.

Although the simulated H<sub>2</sub> isotherms of both NU-100SP and NU-100 are in very good overall agreement with the experimental H<sub>2</sub> measurements (Fig. 4, Table 2), the experimental uptake at high pressure is less than the ideal calculated uptake. The presence of solvent molecules and/or defects (such as collapsed cavities) in NU-100 may partially account for such differences, as simulations were conducted with solvent- and defect-free structures. However, considering the successful activation of NU-100, such pore damage is likely to be minor. Limitations in the molecular model are another possible explanation for the deviations encountered at high pressures. In particular, the strength of the H<sub>2</sub>–H<sub>2</sub> interactions may be overestimated in the simulations, because there is nearly perfect agreement between experimental and simulated H<sub>2</sub> uptake data at lower pressure where framework–H<sub>2</sub> interactions dominate. One additional factor may be the neglect of quantum diffraction effects for the light H<sub>2</sub> molecules at 77 K. Indeed, based on studies by Johnson and colleagues<sup>38</sup>, this is probably the most important effect, likely contributing a 10–15% difference between experimental and computationally modelled values for hydrogen uptake.

Carbon dioxide sorption measurements reveal a high CO<sub>2</sub> storage capacity for NU-100 at 40 bar (excess = 2,043 mg g<sup>-1</sup> and total = 2,315 mg g<sup>-1</sup>). Because of their large pore sizes, NU-100 and related MOFs are not suited for CO<sub>2</sub> capture from sources such as flue gas, where the typical anticipated partial pressure of CO<sub>2</sub> is 0.1 bar (ref. 39). However, at 40 bar and 298 K, conditions potentially relevant for storage, NU-100 displays one of the largest values yet reported for a MOF material (Table 1). The simulated isotherms show excellent agreement with the experimental data, and even capture the inflection behaviour of the experimental isotherms, but slightly underestimate CO<sub>2</sub> uptake at low pressure (Table 2, Fig. 4c). This discrepancy at low pressure is expected, because CO<sub>2</sub> molecules can form weak coordination bonds with the open copper sites via interactions that are not represented in our classical molecular model (that is, those between the lone pairs of the oxygen atom of CO<sub>2</sub> and the unfilled valence orbitals of the metal ions). Once the open sites are fully occupied by CO<sub>2</sub> molecules, the model yields very good agreement with the experimental CO<sub>2</sub> isotherm.

The stability of NU-100 was confirmed in three ways. First, TGA measurements revealed that NU-100 can be fully evacuated and

**Table 2 | Experimental and simulated surface areas and gas sorption data for NU-100 and NU-100SP.**

	BET SA (m <sup>2</sup> g <sup>-1</sup> )	Excess H <sub>2</sub> uptake* (mg g <sup>-1</sup> )	Total H <sub>2</sub> uptake <sup>†</sup> (mg g <sup>-1</sup> )	Excess CO <sub>2</sub> uptake <sup>‡</sup> (mg g <sup>-1</sup> )	Total CO <sub>2</sub> uptake <sup>§</sup> (mg g <sup>-1</sup> )
NU-100SP (simulated)	6,605	121	191	2,017	2,311
NU-100 (simulated)	6,515	125	198	2,129	2,432
NU-100 (experiment)	6,143	99.5	164	2,043	2,315

\*Maximum value at 77 K. <sup>†</sup>At 70 bar and 77 K. <sup>‡</sup>Maximum value at 298 K. <sup>§</sup>At 40 bar and 298 K. SA, surface area.

resolvated (Fig. 2a). Second,  $N_2$  adsorption measurements were repeated five times, and showed negligible change between runs 1 and 5 (see Supplementary Information). Third, high-pressure  $H_2$  uptake was repeated three times; runs 1 and 3 were found to be the same, within experimental error for the instrument (see Supplementary Information). These tests show that NU-100 can be fully evacuated and filled with  $H_2$  at 70 bar, multiple times, and with no evidence of degradation.

In conclusion, the utility of NU-100 as a benchmark material with high surface area and excellent high-pressure  $H_2$  and  $CO_2$  storage capacities has been demonstrated. This material was obtained using a *de novo* approach entailing computational design and simulations before experimentation. The experimental data for NU-100 and the simulated data generated from both NU-100SP and NU-100 are in excellent agreement. We envisage that this approach will be useful in the synthesis of many new MOF structures with improved properties, for a variety of applications.

Received 23 June 2010; accepted 29 July 2010;  
published online 12 September 2010

## References

- Ferey, G. Hybrid porous solids: past, present, future. *Chem. Soc. Rev.* **37**, 191–214 (2008).
- Yaghi, O. M. *et al.* Reticular synthesis and the design of new materials. *Nature* **423**, 705–714 (2003).
- Horiike, S., Shimomura, S. & Kitagawa, S. Soft porous crystals. *Nature Chem.* **1**, 695–704 (2009).
- Sava, D. F. *et al.* Exceptional stability and high hydrogen uptake in hydrogen-bonded metal–organic cubes possessing ACO and AST zeolite-like topologies. *J. Am. Chem. Soc.* **131**, 10394–10396 (2009).
- Lin, X. *et al.* High capacity hydrogen adsorption in Cu(II) tetracarboxylate framework materials: the role of pore size, ligand functionalization and exposed metal sites. *J. Am. Chem. Soc.* **131**, 2159–2171 (2009).
- Murray, L. J., Dinca, M. & Long, J. R. Hydrogen storage in metal–organic frameworks. *Chem. Soc. Rev.* **38**, 1294–1314 (2009).
- Kaye, S. S., Dailly, A., Yaghi, O. M. & Long, J. R. Impact of preparation and handling on the hydrogen storage properties of  $Zn_4O(1,4\text{-benzenedicarboxylate})_3$  (MOF-5). *J. Am. Chem. Soc.* **129**, 14176–14177 (2007).
- Furukawa, H., Miller, M. A. & Yaghi, O. M. Independent verification of the saturation hydrogen uptake in MOF-177 and establishment of a benchmark for hydrogen adsorption in metal–organic frameworks. *J. Am. Chem. Soc.* **129**, 3197–3204 (2007).
- Koh, K., Wong-Foy, A. G. & Matzger, A. J. A porous coordination copolymer with over 5,000  $m^2/g$  BET surface area. *J. Am. Chem. Soc.* **131**, 4184–4185 (2009).
- Rosi, N. L. *et al.* Hydrogen storage in microporous metal–organic frameworks. *Science* **300**, 1127–1129 (2003).
- Eddaoudi, M. *et al.* Systematic design of pore size and functionality in isorecticular MOFs and their application in methane storage. *Science* **295**, 469–472 (2002).
- Li, J.-R., Kuppler, R. J. & Zhou, H.-C. Selective gas adsorption and separation in metal–organic frameworks. *Chem. Soc. Rev.* **38**, 1477–1504 (2009).
- Ma, L., Abney, C. & Lin, W. Enantioselective catalysis with homochiral metal–organic frameworks. *Chem. Soc. Rev.* **38**, 1248–1256 (2009).
- Lee, J. *et al.* Metal–organic framework materials as catalysts. *Chem. Soc. Rev.* **38**, 1450–1459 (2009).
- Allendorf, M. D., Bauer, C. A., Bhakta, R. K. & Houk, R. J. T. Luminescent metal–organic frameworks. *Chem. Soc. Rev.* **38**, 1330–1352 (2009).
- Min, K. S. & Suh, M. P. Silver(I)-polynitrile network solids for anion exchange: anion-induced transformation of supramolecular structure in the crystalline state. *J. Am. Chem. Soc.* **122**, 6834–6840 (2000).
- An, J., Geib, S. J. & Rosi, N. L. Cation-triggered drug release from a porous zinc-adeninate metal–organic framework. *J. Am. Chem. Soc.* **131**, 8376–8377 (2009).
- Horcajada, P. *et al.* Metal–organic frameworks as efficient materials for drug delivery. *Angew. Chem. Int. Ed.* **45**, 5974–5978 (2006).
- Düren, T., Bae, Y.-S. & Snurr, R. Q. Using molecular simulation to characterise metal–organic frameworks for adsorption applications. *Chem. Soc. Rev.* **38**, 1237–1247 (2009).
- Han, S. S., Mendoza-Cortes, J. L. & Goddard III, W. A. Recent advances on simulation and theory of hydrogen storage in metal–organic frameworks and covalent organic frameworks. *Chem. Soc. Rev.* **38**, 1460–1476 (2009).
- Walton, K. S. & Snurr, R. Q. Applicability of the BET method for determining surface areas of microporous metal–organic frameworks. *J. Am. Chem. Soc.* **129**, 8552–8556 (2007).
- Wang, X.-S. *et al.* A large-surface-area boracite-network-topology porous MOF constructed from a conjugated ligand exhibiting a high hydrogen uptake capacity. *Inorg. Chem.* **48**, 7519–7521 (2009).
- Nouar, F. *et al.* Supermolecular building blocks (SBBs) for the design and synthesis of highly porous metal–organic frameworks. *J. Am. Chem. Soc.* **130**, 1833–1835 (2008).
- Yan, Y. *et al.* Exceptionally high  $H_2$  storage by a metal–organic polyhedral framework. *Chem. Commun.* 1025–1027 (2009).
- Wang, X.-S. *et al.* Enhancing  $H_2$  uptake by ‘close-packing’ alignment of open copper sites in metal–organic frameworks. *Angew. Chem. Int. Ed.* **47**, 7263–7266 (2008).
- Hu, Y. *et al.* A new MOF-505 analog exhibiting high acetylene storage. *Chem. Commun.* 7551–7553 (2009).
- Frost, H. & Snurr, R. Q. Design requirements for metal–organic frameworks as hydrogen storage materials. *J. Phys. Chem. C* **111**, 18794–18803 (2007).
- Yuan, D., Zhao, D., Sun, D. & Zhou, H.-C. An isorecticular series of metal–organic frameworks with dendritic hexacarboxylate ligands and exceptionally high gas-uptake capacity. *Angew. Chem. Int. Ed.* doi:10.1002/anie.201001009.
- Materials Studio v 5.0. Accelrys Software Inc., San Diego, CA 92121, USA.
- Rappe, A. K., Colwell, K. S., Goddard III, W. A. & Skiff, W. M. UFF, a full periodic table force field for molecular mechanics and molecular dynamics simulations. *J. Am. Chem. Soc.* **114**, 10024–10035 (1992).
- Gelb, L. D. & Gubbins, K. E. Pore size distributions in porous glasses: a computer simulation study. *Langmuir* **15**, 305–308 (1998).
- Nelson, A. P., Farha, O. K., Mulfort, K. L. & Hupp, J. T. Supercritical processing as a route to high internal surface areas and permanent microporosity in metal–organic framework materials. *J. Am. Chem. Soc.* **131**, 458–460 (2008).
- Furukawa, H. *et al.* Ultra-high porosity in metal–organic frameworks. *Science* **329**, 424–428 (2010).
- Latroche, M. *et al.* Hydrogen storage in the giant-pore metal–organic frameworks MIL-100 and MIL-101. *Angew. Chem. Int. Ed.* **45**, 8227–8231 (2006).
- Yong, Y. *et al.* Metal–organic polyhedral frameworks: high  $H_2$  adsorption capacities and neutron powder diffraction studies. *J. Am. Chem. Soc.* **132**, 4092–4094 (2010).
- <http://webbook.nist.gov/chemistry/fluid/>.
- [http://www.hydrogen.energy.gov/annual\\_progress09.html](http://www.hydrogen.energy.gov/annual_progress09.html).
- Liu, J. *et al.* Adsorption and diffusion of hydrogen in a new metal–organic framework material:  $[Zn(bdc)(ted)_{0.5}]$ . *J. Phys. Chem. C* **112**, 2911–2917 (2008).
- Yazaydin, A. Ö. *et al.* Screening of metal–organic frameworks for carbon dioxide capture from flue gas using a combined experimental and modeling approach. *J. Am. Chem. Soc.* **131**, 18198–18199 (2009).
- Millward, A. R. & Yaghi, O. M. Metal–organic frameworks with exceptionally high capacity for storage of carbon dioxide at room temperature. *J. Am. Chem. Soc.* **127**, 17998–17999 (2005).

## Acknowledgements

The authors gratefully acknowledge support from the Defense Threat Reduction Agency (HDTRA1-08-C-005), the Department of Energy (DE-FG36-08GO18137 and DE-FG02-08ER15967), the National Science Foundation (EEC-0647560) and Argonne National Lab (supercomputing time on Carbon cluster).

## Author contributions

O.K.F. and A.Ö.Y. designed the research. A.Ö.Y. performed the simulations with advice and assistance from R.Q.S. O.K.F. and I.E. synthesized  $LH_6$  with general synthesis advice from S.T.N. O.K.F. synthesized NU-100. O.K.F. and B.G.H. performed the physical measurements. C.D.M. was responsible for solving the crystal structure with assistance from M.G.K. J.T.H. contributed to the development of the general MOF-activation methodology and assisted with data interpretation. All authors discussed the results, contributed to writing the manuscript and commented on it.

## Additional information

The authors declare no competing financial interests. Supplementary information and chemical compound information accompany this paper at [www.nature.com/naturechemistry](http://www.nature.com/naturechemistry). The Cambridge Crystallographic Data Centre deposition number for NU-100 is CCDC 777421. Reprints and permission information is available online at <http://npg.nature.com/reprintsandpermissions/>. Correspondence and requests for materials should be addressed to R.Q.S. and J.T.H.

Reproduced with permission of the copyright owner. Further reproduction prohibited without permission.